ISSN 1573-160X, *PHYSICAL OCEANOGRAPHY*, Vol. 33, Iss. 1, pp. 127-155 (2026)
Original Russian Text © P. N. Lishaev, E. A. Kubryakova, A. A. Kubryakov, 2026,
published in *Morskoy Gidrofizicheskiy Zhurnal*, 2025, Vol. 42, Iss. 1, pp. 115–143

Original article

Modeling the Phytoplankton Dynamics in the Black Sea Based on Calculations of the Three-Dimensional Numerical Physical-Biochemical Model *NEMO-BFM*

P. N. Lishaev ✉, E. A. Kubryakova, A. A. Kubryakov

Marine Hydrophysical Institute of RAS, Sevastopol, Russian Federation
✉ *pavellish@mail.ru*

Abstract
Purpose. The purpose of the work is to study the seasonal, interannual, and spatial variability of key nutrients, chlorophyll a concentration, and phytoplankton species (including large and small diatoms and coccolithophores) dominant in the Black Sea based on numerical modeling.
Methods and Results. Numerical calculations for the period 2008–2014 were performed using the *NEMO-BFM* three-dimensional model adapted to the Black Sea basin. The modeling results made it possible to reproduce the autumn and spring "blooms" of small diatoms, as well as to describe the features of spatial variability of phytoplankton in the Black Sea, particularly the dominance of large diatoms on the basin shelf. After being added to the model, the parameterizations of coccolithophore osmotrophy and dissolved organic matter photodegradation processes permitted the qualitative reproduction of the coccolithophore seasonal variability characteristic of the central Black Sea, namely a summer "bloom" in the upper 20 m layer from late April to July. The model-derived "bloom" begins somewhat earlier than that obtained from *in situ* observations. The resulting spatial variability in the distribution of coccolithophore concentration at the sea surface qualitatively agrees with remote-sensing data. The summer "bloom" is most intense in the central Black Sea, where the phosphate influx from the nutricline to the upper layer is most active. Then the coccolithophore concentration increases towards the continental slope, reaching its highest values there. Moreover, the model has reproduced the winter coccolithophore "bloom", which is weaker as compared to the summer one. The above patterns of coccolithophore variability are consistent with Bio-Argo floats measurements.
Conclusions. The developed *NEMO-BFM* model is a tool that makes it possible to reproduce the spatial variability of chemical and biological substances in the Black Sea and to study their relations with the impact of various physical processes: wind and convective mixing, large-scale and synoptic water dynamics, and propagation of river plumes.

Keywords: Black Sea, numerical modeling, coccolithophores, diatoms, zooplankton, suboxic zone, oxidation-reduction reactions, Bio-Argo floats, chlorophyll *a*, *NEMO*, *BFM*

Acknowledgments: Setting up a three-dimensional biogeochemical *BFM* model for the Black Sea basin, as well as validation of the obtained model results, were carried out within the framework of the state assignment theme of FSBSI FRC MHI FNNN-2024-0012 "Analysis, diagnosis, and operational forecast of the state of hydrophysical and hydrochemical fields of seawater areas based on mathematical modeling using the data of remote and contact measurement methods"; the impact of eddy dynamics on phytoplankton spatial and temporal variability was studied under the RSF grant No. 23-17-00056. The authors are grateful to A.S. Mikaelyan, V.A. Silkin, A.G. Zatsepin, and E.G. Arashkevich for their valuable advice.

For citation: Lishaev, P.N., Kubryakova, E.A. and Kubryakov, A.A., 2026. Modeling the Phytoplankton Dynamics in the Black Sea Based on Calculations of the Three-Dimensional Numerical Physical-Biochemical Model *NEMO-BFM*. *Physical Oceanography*, 33(1), pp. 127-155.

Introduction

The dynamics of biological characteristics of marine ecosystems depend on numerous diverse factors, which include: biological interactions; the variety of physical processes affecting the horizontal and vertical transport of nutrients; variability of light conditions; organic matter remineralization processes. Despite more than 100 years of biological research history in the Black Sea [1] [1], the data on spatiotemporal variability of even the first trophic-level link – phytoplankton – are extremely limited.

In situ biological-chemical measurements are irregular in time and space, often have coarse vertical resolution, and are extremely rare in winter. In recent years, a number of works have described in detail the seasonal variability of ecosystem characteristics, in particular the taxonomic composition of phytoplankton [2–4]. These studies have identified the dominant phytoplankton groups in the Black Sea and proposed several hypotheses regarding the causes of the seasonal succession of these groups. At the same time, a number of authors point to significant high-frequency variability of biological processes associated with the influence of intense wind forcing, synoptic eddies, etc. [5–7]. Optical measurements demonstrate the presence of sharp vertical changes in phytoplankton characteristics, which are difficult to describe using rare *in situ* measurements [5, 8].

New information on the vertical distribution of a number of bio-optical characteristics was provided by Bio-Argo float measurements, which made it possible to obtain regular data on the long-term variability of the vertical evolution of coccolithophore "blooms" [5], light conditions, chlorophyll a concentration [9], and oxygen [10, 11]. It should be noted that chlorophyll a concentration data provide only indirect information on phytoplankton biomass, without the possibility of determining its taxonomic composition. Under conditions of sharp phytoplankton variability, which is clearly visible on the surface from satellite images [12–14], neither *in situ* measurements nor float data allow one to describe the spatial distribution of biological characteristics.

All these factors lead to the necessity of developing new research tools – physical-biochemical models. Work on modeling the Black Sea ecosystem dynamics began in the 1980s [2, 3] [15–17]. In [18–21], the seasonal variability of plankton species was described based on a one-dimensional model. In [20–25], estimates of the variability of the average vertical structure of a number of biological characteristics, e.g., diatom and dinoflagellate "blooms", were obtained using one-dimensional models. The variability of coccolithophore "blooms", which play a significant role in the basin's ecosystem, was analyzed using modeling data in only one work [26].

---

[1] Sorokin, Yu.I., 1982. *The Black Sea: Nature, Resources*. Moscow: Nauka, 217 p. (in Russian).

[2] Belyaev, V.I., 1987. *Modelling of Marine Systems*. Kiev: Naukova Dumka, 201 p. (in Russian).

[3] Vinogradov, M.E., 1989. Dynamic Models of Pelagic Ecosystems. In: K. N. Nesis, ed., 1989. *Models of Oceanic Processes*. Moscow: Nauka, pp. 252-259 (in Russian).

Three-dimensional models were used to describe the Black Sea ecosystem in a limited number of studies [23, 27, 28]. In [27], the influence of warming conditions in 1971–2001 on the intensity of the spring phytoplankton "bloom" was investigated. In [23], within the framework of a three-dimensional model, exchange processes between the waters of the shelf, continental slope, and central part of the Black Sea were considered, and the nitrogen balance on the shelf and in the continental slope area was assessed. In [28], changes in the Black Sea ecosystem as a result of eutrophication were studied, with special focus on biogeochemical processes in the anaerobic zone.

The functioning of the ecosystem modeled in most of these works was based on a single element – nitrogen – limiting phytoplankton growth. However, phosphates can play an extremely important role during phytoplankton "blooms" [4, 29]. They may be the most important limiting element in the central part of the sea, where the Redfield ratio is significantly less than 16 [30]. This is associated with intensive redox processes in the suboxic zone, the description of which poses a certain challenge for modeling. Denitrification processes in this zone can have a significant impact on the dynamics of nitrogen compounds. Modeling the suboxic and hydrogen sulfide zones in the Black Sea, initiated in works [4] [15, 16, 21, 28, 31–33], has a long history. According to recent results, Mn and Fe compounds have a significant effect on oxidation processes in the suboxic zone, causing a decrease in nitrate flux [21, 28, 31–33].

In the present work, for the first time, an adapted three-dimensional *NEMO-BFM* model, which accounts for the cycles of nitrogen, phosphorus, and carbon, is used to describe the long-term variability of the Black Sea ecosystem. The *BFM* model has previously been successfully applied to model the variability of ecosystems in areas such as the White Sea, Baltic Sea, and Mediterranean Sea [34–37]. Reactions were included in the model to reproduce coccolithophore "blooms" (photodegradation of dissolved organic matter (DOM) to a labile state under solar radiation, as well as coccolithophore uptake of labile DOM) and redox reactions in the suboxic zone. To describe the evolution of physical fields, the *NEMO* model was employed, which has been widely used recently to study the Black Sea physics at various spatial scales [38, 39].

The work is aimed at studying, at various temporal and spatial scales, the variability of the main nutrients, chlorophyll a concentration, and phytoplankton species dominant in the Black Sea based on numerical modeling data.

Materials and methods

Hydrodynamic block

We applied the *NEMO* model [40, 41] to reconstruct the hydrodynamics of the Black Sea waters. The grid resolution on a regular grid is 1/10° in the meridional

[4] Sovga, E.E., 2002. [*Features of the Functioning Mechanisms of the Black Sea Shelf and Pelagic Ecosystems*]. Thesis DSc. (Geogr.). Sevastopol, 308 p. (in Russian).

and zonal directions. Vertically, 65 horizons with non-uniform spacing were specified. To describe the fine vertical structure in the upper 200 m layer, the spacing between vertical horizons was set by a special function and varied as follows: 1.25, 3.75, 6.25, ..., 80, 83, ..., 95, 99, 103, 107, 112, 117, 123, 130, 138, 147, 158, 171, 186, and 205 m. Atmospheric forcing fields were taken from the ERA5 reanalysis [42] for 2008–2014.

Parameterization of main biological processes

The *BFM* model [43] includes three groups of living organisms (phytoplankton, zooplankton, and bacterioplankton), each described by a set of differential equations, the number of which depends on the set of elements (C, N, P, Si, Fe, and *Chl*) involved in the life processes of the groups. Each group of living and non-living components of the model can contain a user-selected set of variables – either already included in the initial version of the model, or a completely new set.

The *BFM* equations are described in detail in [43]; each variable is mathematically represented as a multidimensional array containing concentrations expressed in terms of reference chemical elements (carbon, nitrogen, phosphorus, etc.). The adapted version of the model resolves equations for three different phytoplankton groups (small and large diatoms, coccolithophores), three zooplankton groups (micro- and mesozooplankton, the latter further divided into omnivorous and carnivorous types), bacterioplankton, as well as inorganic variables (phosphates, nitrates, ammonium, silicates, oxygen, carbon dioxide, hydrogen sulfide, etc.). The phytoplankton groups were selected according to the results of detailed phytoplankton studies presented in [2–4]. It is noted that dinoflagellates are not accounted for in the current version of the model. The functioning of the ecosystem within the proposed model is limited by nitrogen and phosphorus availability. Initial conditions for the biological block assume equal low concentrations (0.005 mmol/m^3) of all components down to a depth of 50 m; below this depth, values are zero.

The relationship between physical and biogeochemical parameters is implemented explicitly through advective terms associated with the current velocity field, as well as diffusive terms. Additionally, there is a relationship between the rate of biological reactions, sea surface irradiance, and ambient temperature. The temperature regime regulates several physiological processes, and in the model this dependence is represented as a coefficient of the following form:

$$f^T = Q_{10}^{\frac{T-10}{10}},$$

where $Q_{10} = 2.5$ is a coefficient depending on the type of functional group.

Photosynthetically active radiation (PAR) penetrating into the depths of the marine environment is parameterized in the model according to the Lambert–Beer formulation. The shortwave radiation flux is taken from the atmospheric

forcing fields (ERA5). As light propagates in water, it is absorbed by suspended particulate matter, background water absorption, and biological particles. A parameterization for light attenuation by dissolved organic matter, which was absent in the original version, was added to the model:

$$I = \varepsilon_{\mathrm{PAR}} Q_S \exp^{\lambda_w z + \int_z^0 \lambda_{\mathrm{bio}}(z')dz'}, \quad (1)$$

where $\varepsilon_{\mathrm{PAR}}$ is available fraction of solar radiation for photosynthesis; Q_S is shortwave radiation (taken from the atmospheric forcing (ERA5) used in the hydrodynamic model); λ_w is the background water absorption coefficient; λ_{bio} is the light absorption coefficient including biological components (chlorophyll a concentration in each phytoplankton group, detritus, DOM); z is depth.

Based on literature data [44] and Bio-Argo float measurements [9], the background PAR attenuation coefficient for Black Sea waters (0.08 1/m), the light attenuation coefficient by dissolved organic matter (0.05 1/m), and the light absorption coefficient by chlorophyll a (0.1 1/m) were selected.

Biological reactions in ecological modeling are usually written as differential equations, with the right-hand side representing the main biogeochemical processes. For example, for phytoplankton the general equation is as follows:

$$\frac{dP}{dt} = Uptake - Exudation - Lysis - Respiration - Grazing, \quad (2)$$

where $\frac{dP}{dt}$ is the change in phytoplankton concentration over time.

Each phytoplankton group is described by identical primitive equations, which differ in the values of physiological parameters. In the model, phytoplankton is described through six elements (C, N, P, Si, Fe, *Chl*) and a differential equation exists for each of them.

Photosynthesis is controlled by an equation including dependence on penetrating sunlight, water temperature, and a constant determining the maximum phytoplankton productivity at 10 °C:

$$P = p\_sum \cdot \exp\left(\log(p\_q10) \cdot \frac{T-10}{10}\right) \cdot \left(1 - \exp\left[-\alpha^B I \Big/ P_S^B\right]\right) \cdot \exp\left[-\beta I \Big/ P_S^B\right], \quad (3)$$

where p_sum is the maximum photosynthesis rate; p_q10 is phytoplankton productivity at 10 °C; α^B is the coefficient responsible for the initial slope of the P-E curve; β is the coefficient responsible for photoinhibition; T is water temperature; I is the light flux.

It is noted that a term accounting for photoinhibition of the photosynthesis process [45], which was absent in the original version, was added to the model. The constants included in the photosynthesis parameterization are given in Table 1; parameter values were taken from an analysis of a series of experimental calculations, which used value ranges from literature sources [3, 43, 46–51].

Table 1

Coefficients for the equation of state of various groups of phytoplankton (P_1 – small diatoms, P_2 – coccolithophores, P_3 – large diatoms)

Parameter	P_1	P_2	P_3
Coefficient Q_{10}(*p_q*10)	2.0	2.0	3.0
Maximum rate of photosynthesis (*p_sum*), 1/day	2.0	2.0	1.0
Respiratory rate at 10 °C (*p_srs*), 1/day	0.01	0.15	0.01
Maximum lysis rate at extreme nutrient concentrations (*p_sdmo*), 1/day	0.05	0.35	0.01
Isolated fraction of primary production (*p_pu_ea*)	0.2	0.4	0.05
Active respiration (*p_pu_ra*)	0.1	0.25	0.1
Absorption coefficient of labile DOM by phytoplankton (*p_suhpR2c*)	0	1.1	0.6
Cell throughput for N (*p_qun*), m^3/mgC/day	0.25	0.025	0.025
Cell throughput for P (*p_qup*), m^3/mgC/day	0.025	0.25	0.025
Coefficient of increase in fat reserves (*p_xqp*)	2.0	2.0	10.0
α^B (initial slope of curve P-E) (*p_alpha_chl*), mgC m^2/mgChl W	0.15	0.12	0.1
β (parameter characterizing photoinhibition) (*p_betta_chl*), mgC m^2/(mgChl h W)	0.015	0	0.007
Ratio of chlorophyll a and carbon contents in a cell [43] (*p_qlcPPy*), mgChl/mgC	0.025	0.02	0.007

Chlorophyll a (*Chl*) concentration in the model is calculated as follows:

$$Chl = p\_qlcPPy(i) \cdot P_c(i),$$

where $p\_qlcPPy(i)$ is the ratio of chlorophyll a to C content in the cell [mgChl/mgC] for each *i*-th phytoplankton type from [43]; $P_c(i)$ is phytoplankton concentration in carbon units.

The main competitive advantage of small diatoms in the model lies in their high rate of nutrient uptake and high growth rate. For large diatoms, the main feature is their low mortality rate, associated with the ability to accumulate fats, and low consumption by zooplankton. As a result, this phytoplankton type is less susceptible to changes in environmental characteristics – light and nutrient availability. At the same time, it is characterized by a relatively low growth rate. Additionally, a term accounting for DOM uptake was added to the model for large diatoms, which also contributes to their growth.

The zooplankton parameterization is taken from works [52, 53]. For zooplankton, the "cannibalism" process is included, i.e. predation on members of its own functional group. Zooplankton is described by growth processes through uptake and losses through excretion, mortality, respiration, and predation by other groups. Each living zooplankton group is described by three functional groups consisting of nitrogen, carbon, and phosphorus. The total amount of food available for a zooplankton species is calculated considering the set of possible "prey". Table 2

shows the consumption coefficients of one species by another, obtained through tuning based on analysis of numerical experiments and literature sources [54–56].

From Table 2, it is evident that large and small diatoms are mainly grazed by mesozooplankton (Z_2), whereas coccolithophores are the primary food for microzooplankton (Z_3). The availability of a particular species for zooplankton is determined by the "prey" quality and mainly depends on its nominal size (the larger the presumed "prey", the less "edible"/qualitative it is). Bacterioplankton (B) is consumed only by microzooplankton, while carnivorous mesozooplankton (Z_1) feeds on its own species and omnivorous mesozooplankton (Z_2).

Table 2

Consumption coefficients of one species by another

Victim	Predator		
	Z_1	Z_2	Z_3
P_1	0.0	1.0	0.05
P_2	0.0	0.1	03
P_3	0.0	0.7	0.0
B	–	–	0.4
Z_1	0.2	0.0	–
Z_2	2.0	1.0	–
Z_3	0.0	0.2	1.0

The equations for bacterioplankton are written analogously to those for phytoplankton and zooplankton groups. Bacterioplankton is described by three differential equations for C, N, and P [57, 58], which also account for anaerobic processes and denitrification. The main carbon source for bacterioplankton is the pool of organic substances consisting of suspended detrital particles and DOM.

Improvement of the *BFM* model for describing coccolithophore "blooms"

According to literature and field data, the development of coccolithophores in the Black Sea begins after the spring diatom "bloom" in May – June in waters depleted of nutrients [1] [29]. These algae develop in the upper layer during the period of maximum irradiance and a thin upper quasi-homogeneous layer (UQL), when intense radiation suppresses chlorophyll a formation in the cells of most other phytoplankton species due to photoinhibition [59]. To exist in this layer, coccolithophores produce a larger number of calcareous coccoliths, protecting them from excessive solar radiation. However, during this period the upper layer contains very low concentrations of inorganic nitrogen, i.e. few available nutrients.

Among the possible causes for coccolithophore development during this period, their ability to consume dissolved organic matter – osmotrophy – is highlighted [60, 61]. DOM is released in large quantities during metabolic activity and as a result

of the die-off of small diatoms. The released DOM is further transformed under the influence of various physical processes. We assume that under the effect of intense radiation in the upper layer, DOM photodegrades to a labile state [62].

To describe this process, a term was added to the phytoplankton equation:

$$\left.\frac{dP_n}{dt}\right|_{\text{bio}} = \sum_{j=3,4} \left.\frac{dP_n}{dt}\right|_{N^j}^{\text{upt}} - \sum_{j=1,6} \left.\frac{dP_n}{dt}\right|_{R_n^{(j)}}^{\text{lys}} - \frac{P_n}{P_c}\sum_{k=2,3} \left.\frac{dP_c}{dt}\right|_{Z_c^{(k)}}^{\text{prd}} + R\left(P_n^i\right), \quad (4)$$

where N^3 are nitrates; N^4 is ammonium; $R_n^{(1)}$ is dissolved organic matter; $R_n^{(6)}$ is detritus; $Z_c^{(k)}$ is zooplankton (the range of numbers for *j* and *k* is shown under the summation sign for each term); $R\left(P_n^i\right)$ is a source of phytoplankton growth upon uptake of labile DOM:

$$R\left(P_n^i\right) = insw\_vector(p\_xqn \cdot p\_qncPPy(i) \cdot [P_c(i) - P_n(i)]),$$

where $insw\_vector$ is a function equal to unity when the argument is greater than zero and equal to zero otherwise; p_xqn is a coefficient of increase in fat reserves; $p\_qncPPy(i)$ is the N:C content ratio in the *i*-th phytoplankton species; $P_c(i), P_n(i)$ are the concentrations of the *i*-th phytoplankton group in carbon/nitrogen units.

In the upper layer, under the effect of solar radiation during photodegradation, DOM becomes labile (LDOM). To describe this process, the equation for DOM was supplemented with the term R_{photo}:

$$\left.\frac{dDOM_i}{dt}\right|_{\text{bio}} = \sum_{j=1}^{3} \left.\frac{dP_i^{(j)}}{dt}\right|_{DOM_i}^{\text{exu}} - \left.\frac{DOM_i}{DOM_c}\frac{dB_c}{dt}\right|_{DOM_c}^{\text{upt}} + \sum_{k=2,3} \left.\frac{Z_i^{(k)}}{Z_c^{(k)}}\frac{dZ_c^{(k)}}{dt}\right|_{DOM_c}^{\text{rel}} + R_{\text{photo}}, \quad (5)$$

where *i* is NO_3, PO_4; *j* = 1, 2, 3; *k* = 2, 3 (indices); R_{photo} is DOM transition into labile organic matter at irradiance values above 200 W/m^2:

$$R_{\text{photo}} = k_1 \cdot DOM_{\text{N}} \cdot r_1,$$

where $k_1 = 0.03$ is a coefficient; $r_1 = \max\left(0, \frac{I}{I_{\min}} - 1\right)$ is a limiting factor; I is irradiance; W/m^2, $I_{\min}$ is the minimum irradiance at which the photodegradation process begins.

Parameterization of processes in the suboxic zone

One of the features of the Black Sea is the presence of a suboxic zone, for the description of which a parameterization of redox reactions was included in the *BFM* model. These processes significantly affect the transformation of all inorganic nitrogen compounds.

At the sea surface, substance fluxes are absent, except for the oxygen flux, which is specified as follows:

$$O_2^{\text{flux}} = f \cdot ([O_2^{\text{sat}}] - [O_2]), \quad (6)$$

where f is a function depending on wind speed and the Schmidt number (ratio between kinematic viscosity and molecular diffusion); O_2^{sat} is the oxygen saturation concentration, calculated from temperature and salinity values [63].

A number of works are devoted to the study of oxidation-reduction processes in the Black Sea [5] [21, 32, 64]. In the model, the parameterization of such processes was set, according to [33], by the following equations:

$$2Mn^{2+} + O_2 + 2H_2O \rightarrow 2MnO_2 + 4H^+, \quad (7)$$

$$5Mn^{2+} + 2NO_3^- + 4H_2O \rightarrow N_2 + 5MnO_2 + 8H^+, \quad (8)$$

$$HS^- + \frac{1}{2}O_2 + H^+ \rightarrow S^0 + H_2O, \quad (9)$$

$$2NH_4^+ + 3MnO_2 + 4H^+ \rightarrow N_2 + 3Mn^{2+} + 6H_2O, \quad (10)$$

$$HS^- + MnO_2 + 3H^+ \rightarrow S^0 + Mn^{2+} + H_2O. \quad (11)$$

Initial fields of oxygen (O_2), phosphates (PO_4^-), nitrates (NO_3^-), manganese (Mn^{2+}), ammonium (NH_4^+), and hydrogen sulfide (HS^-) are set according to data [5] [65] and values from the MHI database [66] considering the initial density field.

The coefficients for the equation of the calculated phytoplankton groups are given in Table 1.

Results and discussion

Validation of hydrodynamic model results

To assess the performance of the coupled model hydrodynamic block, we consider the diagrams of interannual and seasonal variability of temperature, averaged over the basin area (Fig. 1, *a*, *b*). As can be seen, over the calculation period 2008–2014, the model reproduces the cold intermediate layer (upper boundary 35–45 m, lower boundary 80–85 m), as well as summer warming with maximum temperature values in August (average seasonal values of 25 °C) and winter cooling (January – March).

The model also successfully reproduces the features of the basin's water dynamics. Note the presence of a strong Rim Current in spring, as well as individual anticyclonic eddies (Sevastopol and Caucasian) on its periphery. In the summer season, with a decrease in wind vorticity, the Rim Current disintegrates into individual eddy structures, which agrees with measurement data [67, 68]. Thus, the current fields reconstructed in the model qualitatively reproduce the main water dynamics of the Black Sea.

[5] Kubryakova, E.A., 2019. [*Modeling of Processes of Horizontal and Vertical Transport of Salt and Biogenic Elements in the Black Sea*]. Thesis Cand. Phys.-Math. Sci. Sevastopol, 179 p. (in Russian).

Oxygen, suboxic zone

Oxygen is one of the most important parameters of the sea state, as it enables the existence of living organisms and also determines the intensity of oxidative processes in the marine environment. Examining the seasonal variability of dissolved oxygen, we note that its maximum concentration is observed in February – March in the layer from the surface to 40 m (Fig. 2, *b*).

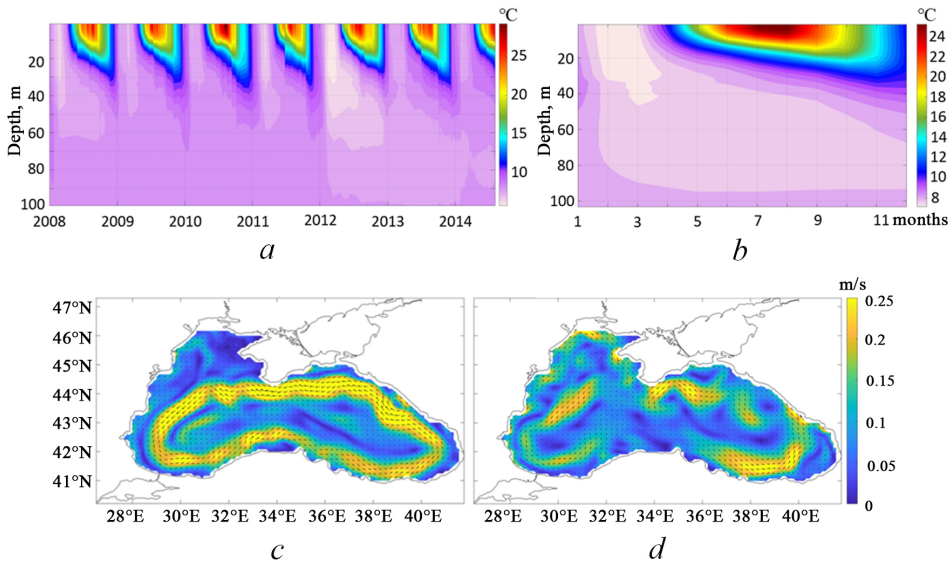

F i g. 1. Interannual and seasonal variability of model temperature (*a*, *b*), and amplitude of current velocities for 27 March (*c*) and 4 July (*d*) 2008

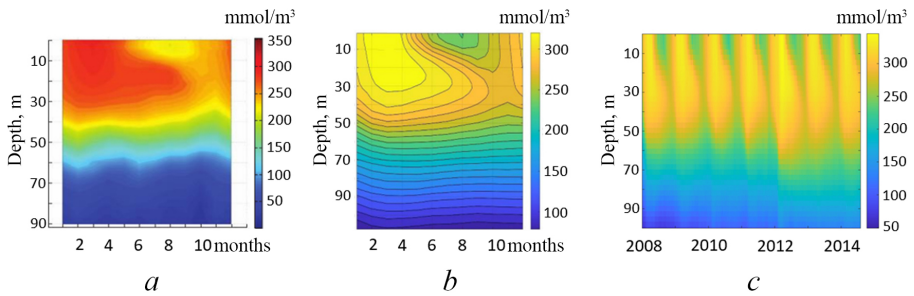

F i g. 2. Seasonal (*a*, *b*) and interannual (*c*) oxygen variability based on Bio-Argo float data (*a*) and numerical modeling (*b*, *c*)

In these months, the average O_2 concentration at the horizon reaches 300 mmol/m^3 (in individual profiles it can be ~ 350 mmol/m^3). Subsequently, the O_2 concentration maximum occupies the subsurface layer of 10–40 m. The subsurface maximum is observed during the spring–summer period and is associated with the photosynthetic activity of phytoplankton. Oxygen concentration

decreases until December and amounts to 260–270 mmol/m^3. It is worth noting the summer subsurface (0–20 m) O_2 concentration minimum (230–240 mmol/m^3) in August– September, when temperature values are maximal. High temperatures lead to a decrease in the solubility of atmospheric oxygen, and phytoplankton growth and biological oxygen production are suppressed under the influence of high PAR values and low nutrient and chlorophyll a content. The seasonal variability of the dissolved oxygen vertical distribution obtained in the model calculation qualitatively coincides with *in situ* measurement data [11, 30] (Fig. 2, *a*). In the interannual variability (Fig. 2, *c*), we note the period after 2012, when the penetration depth of high oxygen concentration values increased on average by 10–15 m (in 2008–2011 the depth of the 250 mmol/m^3 isoline was ~ 55 m, after 2011 – 65–70 m), which agrees with the analysis of Bio-Argo float data [11, 69].

Variability of major nutrient concentrations

The main feature of the interannual and seasonal variability of major nutrient concentrations in the central part of the sea (depths greater than 500 m) is the episodic influx of nitrates into the upper layers in winter (February – March) as a result of vertical entrainment from the nutricline layer (Fig. 3). Such processes are short-term in nature and are associated with the effects of cooling and storms. As a result, nitrate concentrations in the upper layer may increase slightly to 0.01 mmol/m^3, as, for example, in 2012. The most intense nutrient entrainment occurs during cold winters, when the density of the upper layer reaches maximum values. In particular, during the cold winter of 2012 (Fig. 4, *a*), the concentration of entrained nitrates in the upper layer was 20 times higher. Such an intense increase in the concentration of available nutrients was one of the causes for the extremely strong coccolithophore “bloom” that year, which was recorded by satellite data [70].

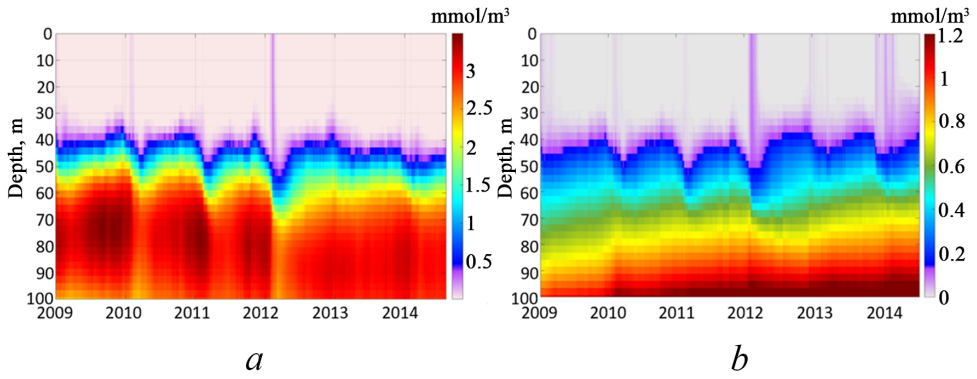

F i g. 3. Interannual variability of the vertical distribution of nitrates (*a*) and phosphates (*b*) in the upper 100 m layer of the central Black Sea

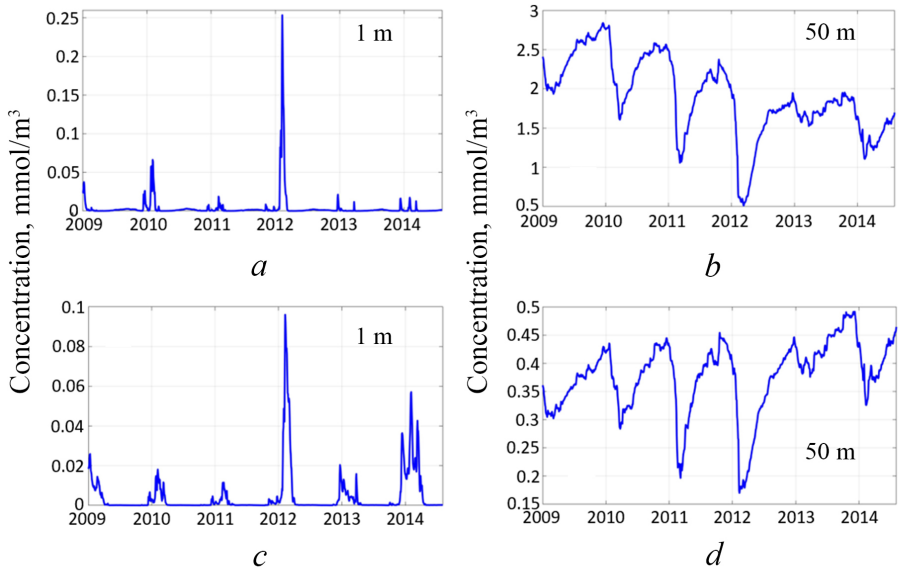

F i g. 4. Temporal variability of nitrate (*a*, *b*) and phosphate (*c*, *d*) concentrations in the central Black Sea

The lower part of the nutricline is characterized by a sharp decrease in NO_3 in the winter–spring period (January – April), caused by its erosion under the effect of vertical mixing. At the same time, NO_3 decreases by a significantly larger amount, 1–1.4 mmol/m^3, which is 10 times higher than its increase in the upper layer. This difference is due to the fact that most of the nutrients entrained into the upper layer are rapidly transformed as a result of phytoplankton consumption and converted into organic form. At the same time, at the end of the year, in the autumn – winter period, a maximum nitrate concentration is observed in the nitracline, i.e. nutrient accumulation occurs, associated with the remineralization of settling organic matter formed during the year.

Similar variability is observed for phosphates (Fig. 3, *b*). They are also characterized by short-term entrainment into the upper layer and a sharp decrease in the nutricline layer (40–60 m) in the spring–winter period. Note, however, that high phosphate concentrations are observed in the upper layer for a longer time. This is due to the fact that in the central Black Sea the N:P ratio is 5–6, which is much lower than the Redfield ratio (16) required for phytoplankton development [30]. As a result, part of the phosphates remains in the upper layer until April – May, when they are actively consumed during the intensive coccolithophore “bloom” [4]. In the shelf part of the sea, due to intense river runoff, an excess of nitrates and a deficiency of phosphates (a high N:P ratio) are observed. This feature may contribute significantly to the functioning of the basin’s ecosystem, in particular to the dynamics of coccolithophore “blooms” on the shelf.

Biological block of the model

Small diatoms (P_1). According to *in situ* measurements, the intense influx of nutrients into the illuminated layers in winter primarily causes rapid growth of small diatoms (P_1) [2], since they possess the highest growth rate. The maximum concentration of small diatoms is observed in February (Fig. 5, 6), when phytoplankton with high concentration values occupies the largest water column (0–50 m). The section in Fig. 6 shows that maximum concentrations are observed in the region of large cyclonic gyres, where the nutricline rises closest to the surface. Another maximum is recorded in the area of the southern continental slope, where nutrients from the northwestern shelf (NWS) are transported during the Rim Current intensification.

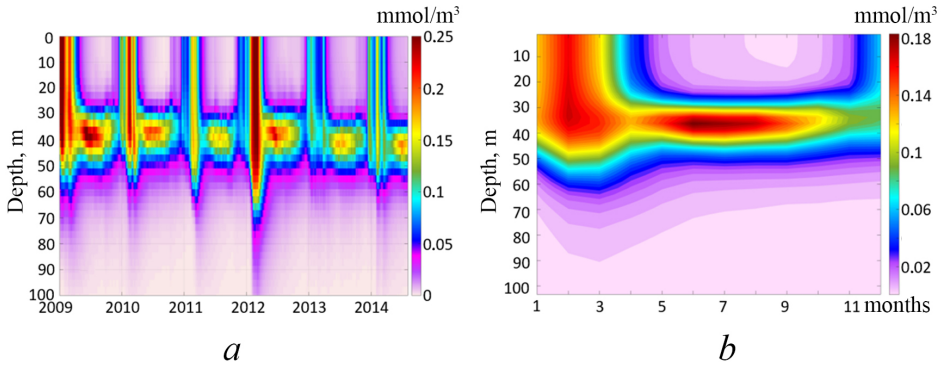

F i g. 5. Interannual (*a*) and seasonal (*b*) variability of the vertical distribution of small diatoms in the upper 100 m layer in the central Black Sea

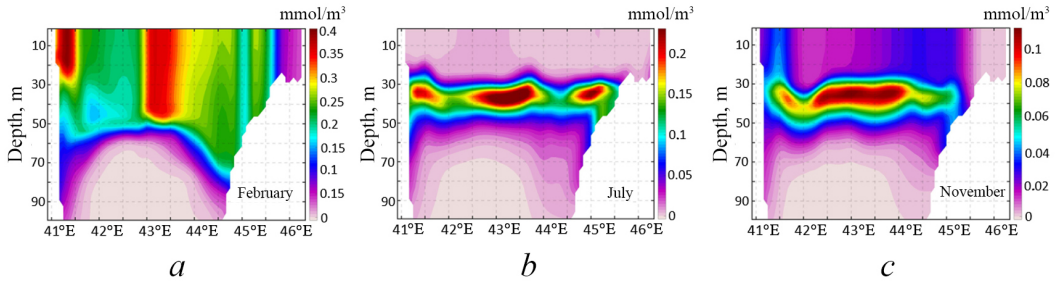

F i g. 6. Concentration of small diatoms along the section through the western cyclonic gyre (31°E) averaged over February (*a*), July (*b*), and November (*c*)

In the summer period, the concentration of diatoms in the upper layer decreases to a seasonal minimum in August, which is associated with a decrease in the amount of available nutrients and excessive irradiance. At this time, high concentrations of diatoms are observed only in the lower part of the euphotic zone (30–40 m), partially determining the development of the summer subsurface chlorophyll a maximum [8, 9]. Nutrients can enter this layer in summer during intense hydrodynamic forcing,

for example after strong storms [5]. The section in Fig. 6, *b* demonstrates that maximum concentrations in summer are observed in the central part of the sea and in the seaward part of the slope.

The UQL deepening and vertical entrainment of nutrients lead to the onset of the autumn “bloom” of small diatoms in the 0–35 m layer in October – November. The UQL increases most sharply in the continental slope area, where stratification is weakened [71]. As a result, as seen in the section of Fig. 6, in this area the entrainment of diatom cells from their subsurface maximum occurs faster, and an initial increase in the concentration of small diatoms at the surface is observed here.

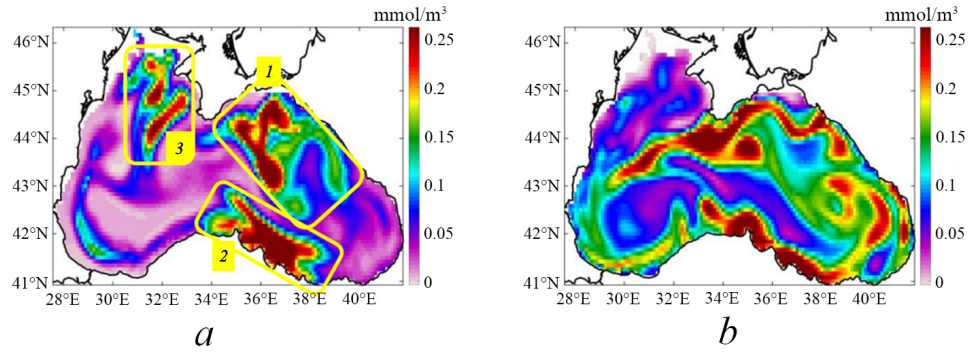

F i g. 7. Significant spatial variability of small diatoms in the area of their subsurface maximum, conditioned by various physical factors, for 14 September 2009 (*a*) and 26 May 2010 (*b*)

Physical factors have a crucial influence on the development of phytoplankton “blooms” and their spatial variability. For example, Fig. 7, a represents a map of the subsurface maximum concentration of small diatoms at the 30 m horizon in mid-September 2009. Three distinct maxima can be distinguished, each associated with a specific process: maximum *1* in the central part – with the action of storms and the vertical uplift of nutrients in the region of cyclonic gyres; maximum *2* in the southern part of the sea – with intense Anatolian upwelling; maximum *3* – with advection of shelf waters from the NWS area under the effect of the Sevastopol anticyclone.

Another example (Fig. 7, *b*) demonstrates an even more complex spatial distribution at a depth of 30 m in May 2010, which is associated both with the influence of vertical advection in synoptic cyclones/anticyclones and with the transport of productive waters in the Rim Current jet from locations of nutrient input under the effect of intense storm activity and coastal upwellings.

DOM and coccolithophores. As a result of lysis and die-off of diatoms in the photic layer, a large amount of dissolved organic nitrogen (DON) is formed. In the present model, the formed DON is partially consumed by bacterioplankton and partially converted into a highly labile form (LDON) under the effect of photodegradation.

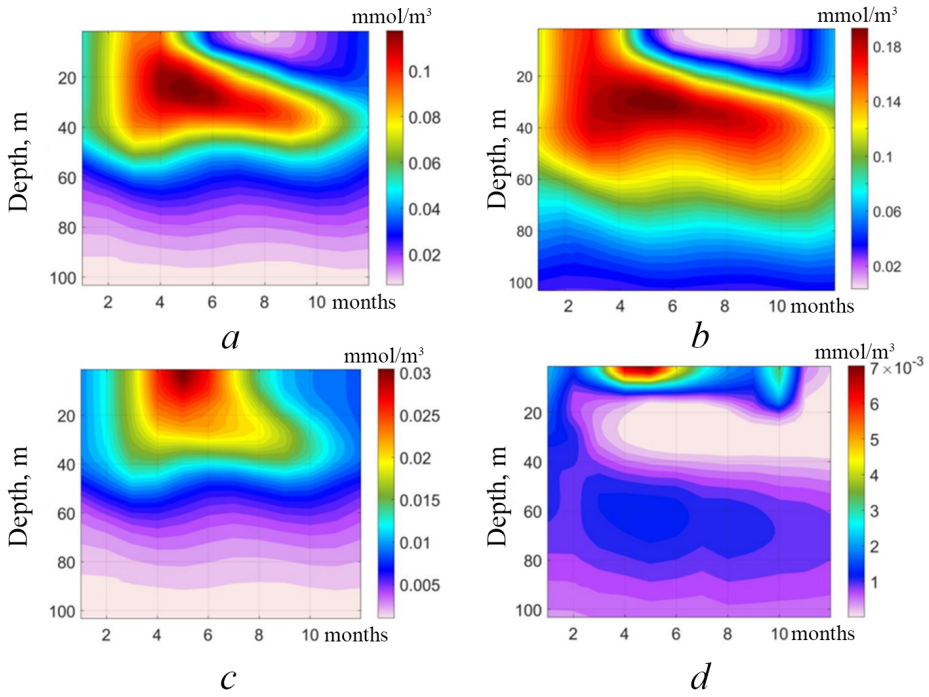

F i g. 8. Seasonal variability of dissolved organic nitrogen (*a*), bacterioplankton (*b*), dissolved organic phosphorus (*c*) and the highly labile form of dissolved organic nitrogen (*d*)

The peak of DON concentration occurs in April – May and is observed in the 10–30 m layer (Fig. 8, *a*). Subsequently, the highest DON concentrations shift to lower layers and are observed in the area of the subsurface phytoplankton maximum at depths of 20–30 m. The main consumer of DON is bacterioplankton; their vertical variability is similar: a maximum is observed in February – April in the 0–50 m layer, with a gradual deepening to depths of 30–40 m occurring in the summer season (Fig. 8, *b*).

In the upper 10 m layer, as a result of intense solar radiation, DON transitions to a highly labile state (Fig. 8, *d*). The transition process takes 1–2 months, and LDON has its highest value in the upper, maximally illuminated layer in April – May. In the present model, LDON is consumed not only by bacterioplankton but also by coccolithophores, as well as large diatoms, as a result of their ability for osmotrophy. Due to the consumption of residual phosphates after winter cooling and LDON in April – May, an intense surface “bloom” of coccolithophores occurs (Fig. 9, *a*, *c*). Note that part of the LDON remains unconsumed and accumulates in the continental slope area, where it subsequently sinks into deeper, non-illuminated layers under the effect of downward motions. This accounts for the LDON maximum at depths of 50–80 m (Fig. 8, *d*).

Such a mechanism for coccolithophore growth agrees with hypotheses proposed earlier in works [4, 29], which note the important role of low N:P ratio and phosphates for coccolithophore “blooms”.

Note that in this calculation the maximum concentration of coccolithophores occurs in April – May (Fig. 9, *b*), which is somewhat earlier than in satellite measurements (May) and direct measurement data (May – June) [72]. The highest concentrations of coccolithophores at the beginning of the “bloom” are observed in the upper 20 m layer, then they gradually deepen (Fig. 9, *b*).

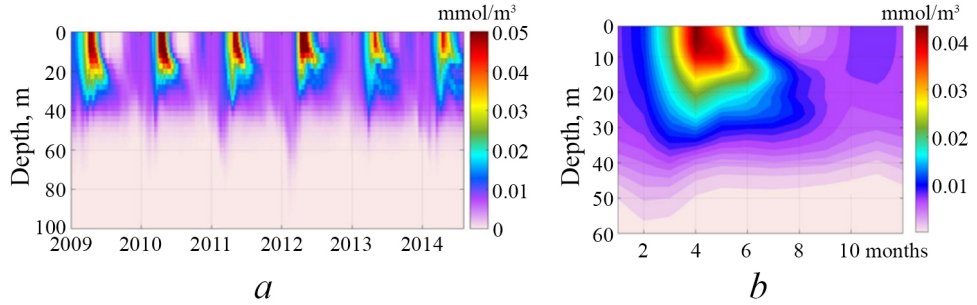

F i g. 9. Interannual (*a*) and seasonal (*b*) variability of the vertical distribution of coccolithophore concentration in the central Black Sea based on the model data

As a result, in July – August the coccolithophore maximum is observed in the subsurface layer at 20–30 m depths. The same process – the beginning of the “bloom” in the upper 20 m layer and gradual subduction into lower layers – is observed in measurements of the backscattering coefficient based on Bio-Argo float data [5].

Satellite measurements show that the summer coccolithophore “bloom” after cold winters is most intense in the central part of the sea. Numerical modeling data successfully reproduce these features – maximum coccolithophore growth in the central cyclonic part of the sea (where phosphates from the nutricline are most actively entrained into the upper layer), as well as their minimum on the NWS (Fig. 10, *a*). At the same time, both data types record relatively low values in the eastern NWS and in the southeastern part of the sea.

Interestingly, as the “bloom” weakens in June – July, its maximum shifts towards the continental slope area and is observed there somewhat later (Fig. 10, *b*, *c*). At this time, favorable conditions for coccolithophore “blooms” arise in the mixing zone of shelf waters and waters of the central part (Fig. 10, *d*). The obtained results agree with satellite measurements. To illustrate the spatial distribution of the coccolithophore “bloom”, MODIS data on the remote sensing reflectance (*Rrs*) at a wavelength of 469 nm were used. The data were obtained from MODIS measurements in the OceanColor archive (http://oceancolor.gsfc.nasa.gov/). Backscattering by coccoliths increases the *Rrs* signal in all optical channels, which is evident in satellite measurements from the MODIS scanner [70]. For example,

brightness maps for 3–4 June 2008 are given in Fig.10, *e*, *g*. Areas of increased brightness values in the central and western parts of the sea and reduced values in the NWS area and the southeastern part of the sea are clearly visible. This distribution qualitatively agrees with the calculation results (Fig. 10, *d*).

After the die-off of coccolithophores, a large amount of dissolved organic phosphorus, which has a seasonal cycle different from DON with a maximum in May in surface layers (Fig. 8, *c*), appears in the water.

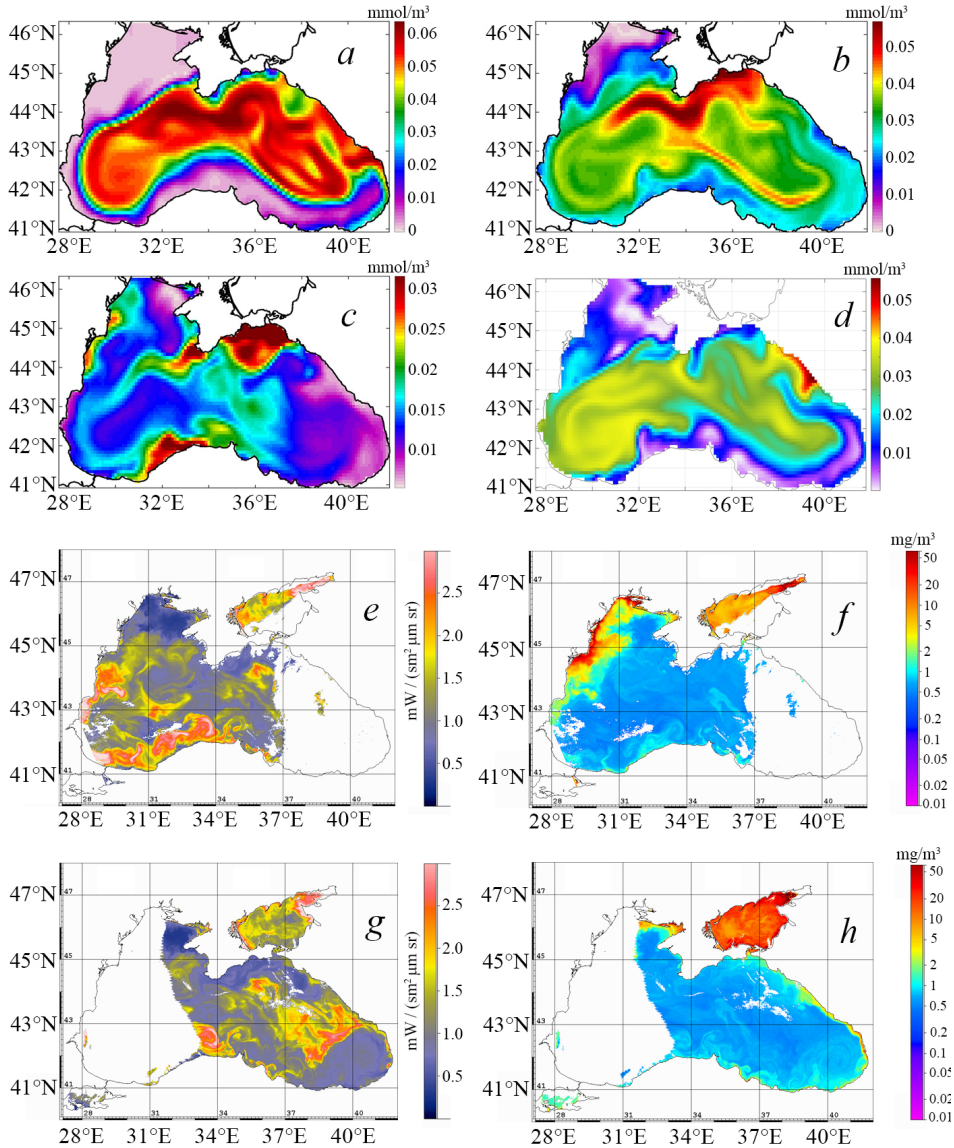

F i g. 10. Coccolithophore concentration based on modeling data at the 25 m horizon (*a–d*); remote sensing reflectance of the sea surface based on MODIS data (*e*, *g*); chlorophyll a concentration based on satellite data (*f*, *h*)

In the Black Sea, not only summer but also a fairly strong autumn – winter coccolithophore “bloom” is observed. Such a “bloom” has been examined in detail; it was observed, in particular, in October 2005 and November 2014 [70]. In these years, and generally according to satellite data, winter coccolithophore “blooms” are more often recorded in the southern part of the Black Sea, less frequently across the entire central part. The proposed model also allows reproducing this second peak, which is identified in the modeling data in October – November (Fig. 11, *c*). At this time, elevated coccolithophore concentrations occupy the entire autumn UQL at depths of 0–40 m, which corresponds to Bio-Argo data [5, 70].

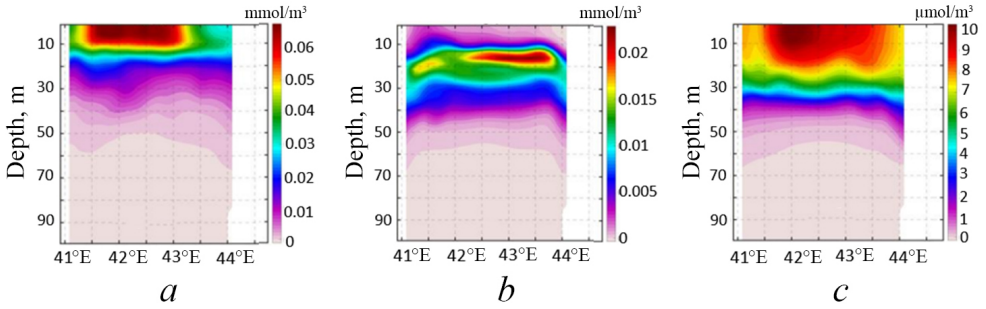

F i g. 11. Distribution of coccolithophore concentration along the section through the eastern cyclonic gyre (39°E) averaged over April (*a*), July (*b*) and November (*c*)

An important cause for such a “bloom” is the export of NWS waters under the influence of the Rim Current. Part of the LDON, intensively formed here in summer, is then transported during the summer-autumn season with the Rim Current to the southern part of the sea. An example of such a process is shown in Fig. 12. During this period, there is an intensification of storm activity (Fig. 12, *c*), which, according to satellite data analysis, is one of the important triggers for winter coccolithophore “blooms”.

Indeed, according to modeling results, such storms in late September 2010 caused the entrainment of phosphates into the upper layer (Fig. 12, *d*). As a result of a large amount of LDON (Fig. 12, *a*) and phosphates in the Rim Current export zone on the continental slope, an autumn-winter coccolithophore “bloom” arose, which is most intense in the southern part of the sea (Fig. 12, *b*). At this time, due to the increase in the UQL, LDON spreads deeper, occupying a larger layer and partially accumulating in the deep layers of the basin.

Large diatom phytoplankton. Another important functional group of phytoplankton in the Black Sea is large diatoms (e.g. *Pseudosolenia calcar-avis*). According to limited *in situ* measurements, this phytoplankton group is most frequently recorded in the coastal zone and in the area of the basin’s continental slope [2]. A similar distribution is obtained from modeling data (Fig. 13, *b*), according to which the maximum concentrations of this phytoplankton group are

concentrated on the NWS and in the Rim Current area, with a minimum observed in the central part of the sea.

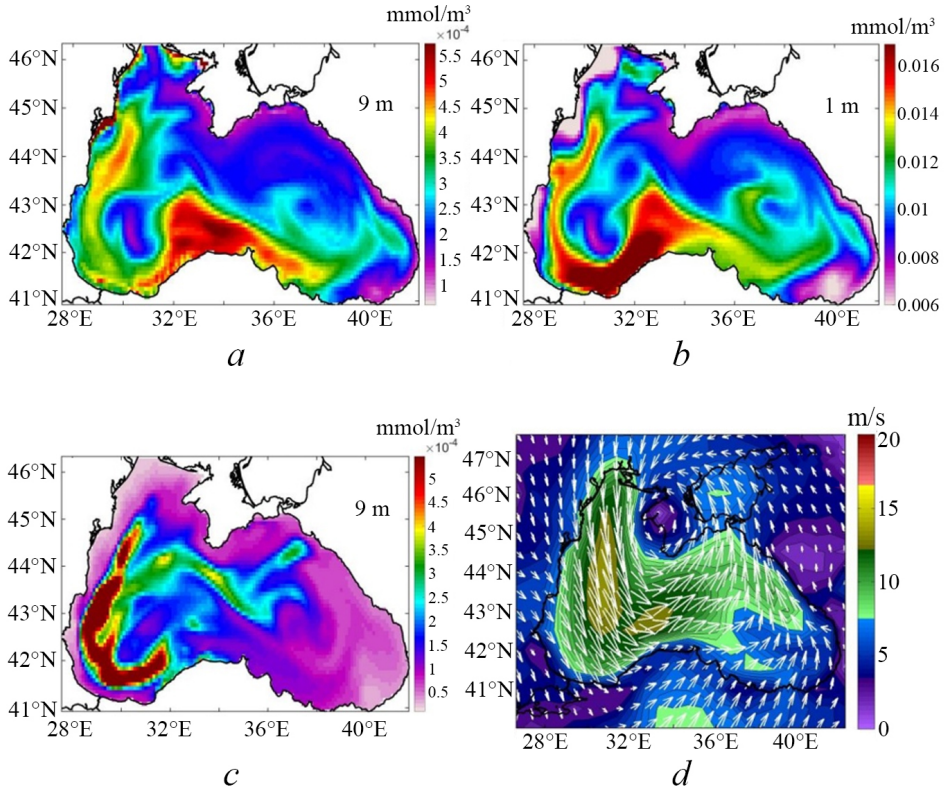

F i g. 12. Development of the winter coccolithophore "bloom" on the southern continental slope in October 2010: monthly mean values of LDON (*a*), coccolithophores (*b*), and phosphates (*c*); wind amplitude and direction on 30 September 2010 (*d*)

For example, Fig. 14 shows the average July concentration of various phytoplankton groups along a section through the western cyclonic gyre. Large diatoms develop most intensively in a thick layer on the continental slope (0–50 m) with a maximum in the lower layers. At the same time, for the other two groups, the most intensive development is characteristic of the central part of the sea: for small diatoms – in the lower part of the euphotic zone (30–50 m), for coccolithophores – at depths of 10–30 m.

According to the modeling results, large diatoms are characterized by a maximum on the continental slope in the summer period in the 10–40 m layer (Fig. 14, *c*), which agrees with field observations [2]. In addition, in some years, for example in 2010, the maximum actively developed in the winter period and occupied a large water column (0–40 m), corresponding to the UQL layer. The minimum for this group is observed in the upper 20 m layer in summer–autumn (Fig. 13, *a*)

(a minimum in the seasonal cycle, but at the same time these values are quite large in absolute terms).

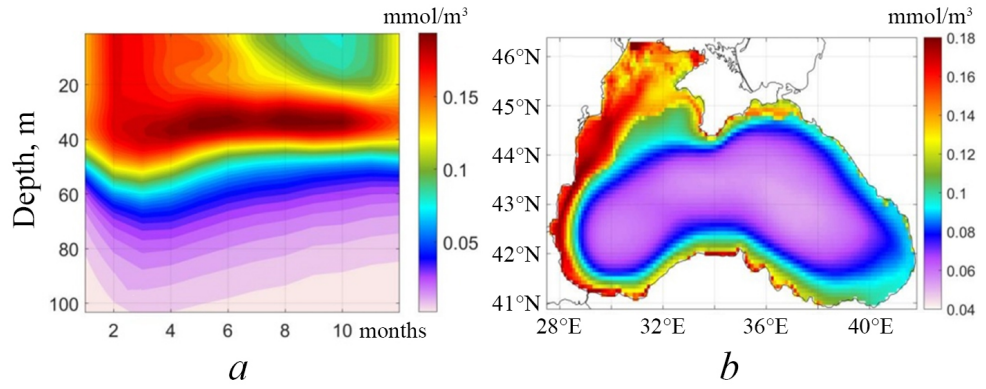

F i g. 13. Averaged seasonal variability of the vertical distribution (*a*) and concentration (*b*) of large diatoms in the 0–100 m layer calculated over the period of the numerical experiment

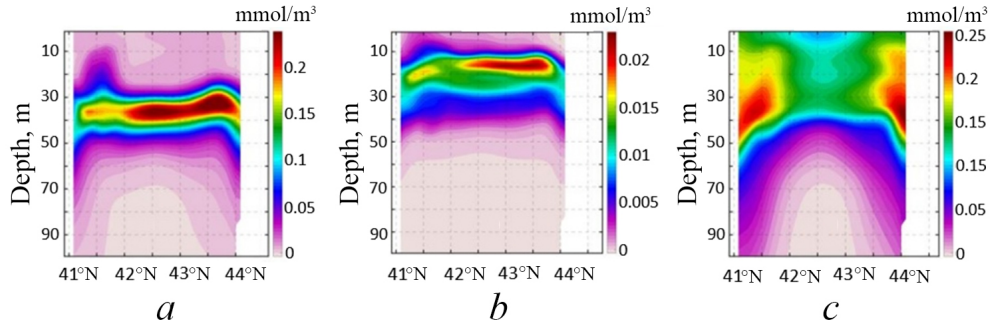

F i g. 14. Concentrations of small diatoms (*a*), coccolithophores (*b*), and large diatoms (*c*) along the section through the western cyclonic gyre (31°E) averaged over July

According to modeling data, the development of large diatoms in the lower part of the euphotic zone on the slope may be caused by the action of two processes: firstly, the impact of downward motions on the transport of nutrients, ammonium, and LDON from shelf areas (in the present model, large diatoms are efficient consumers of ammonium and LDOM, which contributes to their growth in this area); secondly, efficient nutrient entrainment as a result of Rim Current intensification and the large thickness of the UQL on the slope. In the present model, large diatoms have low mortality rates (due to fat reserves) and are less susceptible to changes in irradiance. Therefore, they can exist in winter in the deep part of the continental slope even with a deep UQL, where the growth of other phytoplankton groups is limited.

The transport of shelf waters under the influence of synoptic eddies is an important cause for the penetration of this phytoplankton group into the central part

of the sea. Such a process was recorded by *in situ* measurements in [2], according to which anticyclonic activity led to an increase in phytoplankton concentration in the eastern part of the Black Sea. A similar process is well observed in the modeling data, for example on 11 August and 19 May 2009. Fig. 15, a clearly shows how a large Sevastopol anticyclone in the northwestern part of the sea led to the influx of a large amount of phytoplankton into its central part. In Fig. 15, *b*, the concentration maximum is also observed in the core of an anticyclone, which had previously been actively entraining shelf waters.

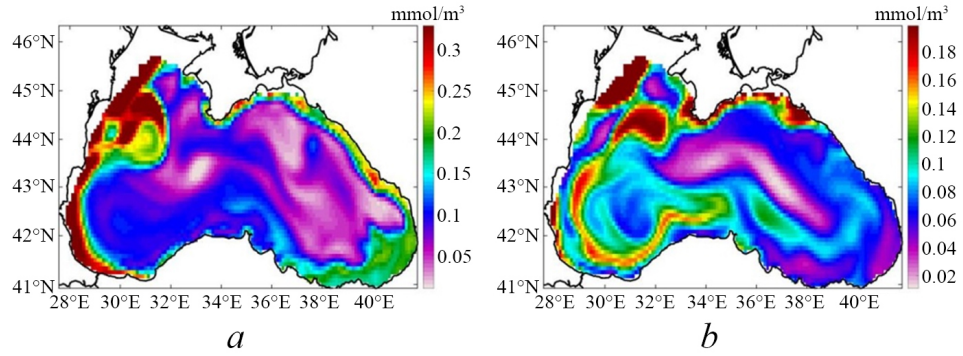

F i g. 15. Impact of synoptic eddies on phytoplankton transport to the central part of the sea. Concentration of large diatoms at the 40 m horizon for 11 August (*a*) and 19 May (*b*) 2009

Chlorophyll a concentration

The vertical variability of chlorophyll a concentration is characterized by an intense maximum in March in the 0–30 m layer, a summer subsurface maximum, and its growth in the upper layer during the autumn period (Fig. 16, 17). Minimum chlorophyll a values are observed in the upper 15 m layer during the warm period of the year, which is associated with nutrient deficiency and the photoinhibition effect. These features, obtained from the model, agree well with field measurements and Bio-Argo float data [9, 73, 74].

The chlorophyll a maximum in March is primarily associated with the development of small diatoms after winter convection. Chlorophyll a values at this time are high in the 0–30 m layer, which agrees with Bio-Argo data. The chlorophyll a increase throughout the water column leads to the seasonal maximum of its integrated concentration. The coccolithophore “bloom” in April – May makes a significantly smaller contribution to the chlorophyll a increase in the upper layer at this time.

The summer subsurface chlorophyll a maximum is determined by the influence of various phytoplankton groups. In the lower part of this maximum (30–50 m), the main contribution comes from small diatoms; this group determines the chlorophyll a concentration in the central part of the sea. In the continental slope area, especially in the deep layers, the main contribution to the development of the chlorophyll a maximum comes from large diatoms. As for small diatoms,

the increase in chlorophyll a in the upper layer during the autumn period is initially recorded in the slope area, where the UQL reaches the position of the chlorophyll a maximum faster and phytoplankton cells are entrained into the upper layer.

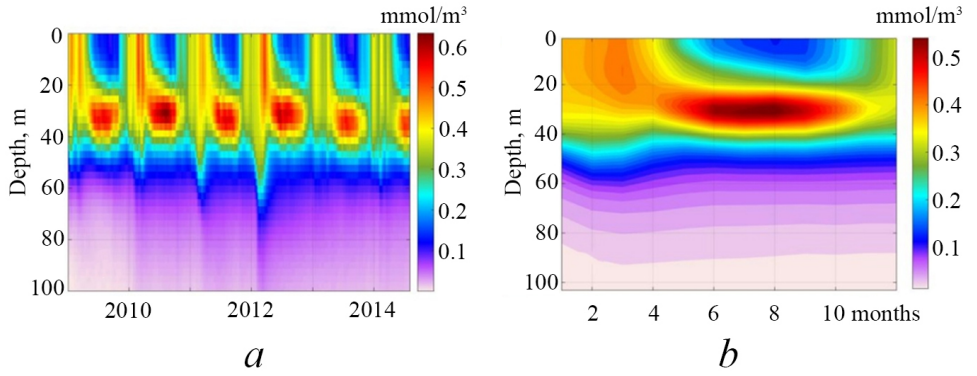

F i g. 16. Interannual (*a*) and seasonal (*b*) variability of chlorophyll *a* concentration in the deep part of the Black Sea based on modeling data

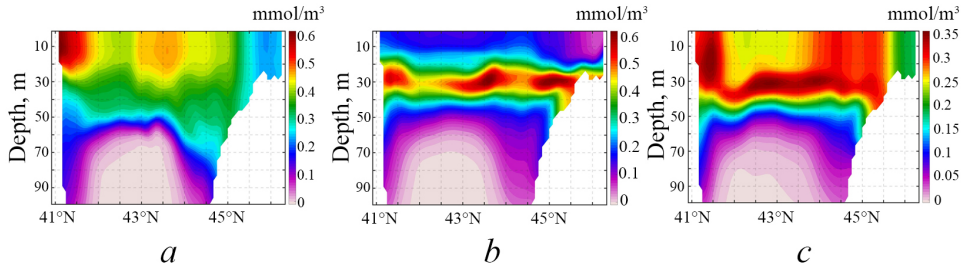

F i g. 17. Chlorophyll *a* concentration along the section through the western cyclonic gyre (31°E) averaged over February (*a*), July (*b*), and November (*c*)

Conclusions

The work presents the results of modeling biochemical processes based on the coupled three-dimensional *NEMO-BFM* model for the Black Sea. The *BFM* model was adapted for the Black Sea and coupled with a previously tuned hydrodynamic *NEMO* model for this region with a resolution of 10 km. One of the Black Sea features is the presence of a suboxic zone, for the description of which redox reactions accounting for oxygen, hydrogen sulfide, and manganese were included in the model. The obtained results for the vertical distribution and seasonal variability of major nutrients, oxygen, and hydrogen sulfide agree with data from previous studies.

The configuration we used includes the calculation of concentrations of large and small diatoms and coccolithophores, which determine the total chlorophyll a concentration in the basin. The selection of these groups is based on studies that analyzed a large statistical array of *in situ* measurements in the northeastern part of the Black Sea. The features of the spatial and temporal variability of chlorophyll

a concentration obtained from numerical modeling data agree well with field measurements and Bio-Argo float data. The modeling results made it possible to reproduce the autumn and spring “blooms” of small diatoms; however, the deep maximum in the lower layers of the photic zone in summer, reproduced in the model, is most likely associated with the absence of other phytoplankton types characteristic of the Black Sea basin (in particular, dinoflagellates)

The modeling data allowed us to describe the dominance of large diatoms on the basin shelf. They develop most intensively on the continental slope in the 0–50 m layer with a maximum at lower horizons. At the same time, in the seasonal cycle, the maximum development of large diatoms occurs in the summer period, which agrees with field observation data.

The features of spatial variability and vertical distribution of coccolithophore “blooms” were reproduced in the model for the first time. For this purpose, the proposed hypothesis about the important role of osmotrophy for their development was applied, i.e. the consumption of dissolved organic matter formed after the spring diatom “bloom”. This hypothesis made it possible to reproduce the seasonal variability of coccolithophore concentration characteristic of the central Black Sea: the “bloom” development from late April to July in the upper 20 m layer. It should be noted that, according to the model, the coccolithophore “bloom” begins somewhat earlier than according to direct observation data. In addition, the model succeeded in reproducing the weaker winter coccolithophore “bloom”, which agrees with Bio-Argo float data.

The model results make it possible to reproduce the significant spatiotemporal variability of chemical and biological substances in the Black Sea associated with the impact of various physical processes.

It should be noted that this model is primarily aimed at reproducing the qualitative characteristics of variability of the first trophic levels of the Black Sea ecosystem. More accurate data require significant efforts to obtain long-term time series of phyto- and zooplankton characteristics, which can be used for tuning such models.

REFERENCES

1. Georgieva, L.V. and Senichkina, L.G., 1996. Phytoplankton of the Black Sea: Current Situation and the Research Prospects. *Ecology of the Sea*, 45, pp. 6-13 (in Russian).
2. Mikaelyan, A.S., Kubryakov, A.A., Silkin, V.A., Pautova, L.A. and Chasovnikov, V.K., 2018. Regional Climate and Patterns of Phytoplankton Annual Succession in the Open Waters of the Black Sea. *Deep Sea Research Part I: Oceanographic Research Papers*, 142, pp. 44-57. https://doi.org/10.1016/j.dsr.2018.08.001
3. Mikaelyan, A.S., Pautova, L.A. and Fedorov, A.V., 2021. Seasonal Evolution of Deep Phytoplankton Assemblages in the Black Sea. *Journal of Sea Research*, 178, 102125. https://doi.org/10.1016/j.seares.2021.102125
4. Silkin, V.A., Pautova, L.A., Giordano, M., Chasovnikov, V.K., Vostokov, S.V., Podymov, O.I., Pakhomova, S.V. and Moskalenko, L.V., 2019. Drivers of Phytoplankton Blooms in the Northeastern Black Sea. *Marine Pollution Bulletin*, 138, pp. 274-284. https://doi.org/10.1016/j.marpolbul.2018.11.042

5. Kubryakov, A.A., Zatsepin, A.G. and Stanichny, S.V., 2019. Anomalous Summer-Autumn Phytoplankton Bloom in 2015 in the Black Sea Caused by Several Strong Wind Events. *Journal of Marine Systems*, 194, pp.11-24. https://doi.org/10.1016/j.jmarsys.2019.02.004

6. Mikaelyan, A.S., Mosharov, S.A., Kubryakov, A.A., Pautova, L.A., Fedorov, A. and Chasovnikov, V.K., 2020. The Impact of Physical Processes on Taxonomic Composition, Distribution and Growth of Phytoplankton in the Open Black Sea. *Journal of Marine Systems*, 208, 103368. https://doi.org/10.1016/j.jmarsys.2020.103368

7. Stanichny, S.V., Kubryakova, E.A. and Kubryakov, A.A., 2021. Quasi-Tropical Cyclone Caused Anomalous Autumn Coccolithophore Bloom in the Black Sea. *Biogeosciences*, 18(10), pp. 3173-3188. https://doi.org/10.5194/bg-18-3173-2021

8. Finenko, Z.Z., Churilova, T.Ya. and Sosik, Kh.M., 2004. Vertical Distribution of Phytoplankton Photosynthetic Characteristics in the Black Sea. *Oceanology*, 44(2), pp. 205-218.

9. Kubryakov, A.A., Mikaelyan, A.S., Stanichny, S.V. and Kubryakova, E.A., 2020. Seasonal Stages of Chlorophyll-a Vertical Distribution and Its Relation to the Light Conditions in the Black Sea from Bio-Argo Measurements. *Journal of Geophysical Research: Oceans*, 125(12), e2020JC016790. https://doi.org/10.1029/2020JC016790

10. Stanev, E.V., He, Y., Staneva, J. and Yakushev, E., 2014. Mixing in the Black Sea Detected from the Temporal and Spatial Variability of Oxygen and Sulfide – Argo Float Observations and Numerical Modelling. *Biogeosciences*, 11(20), pp. 5707-5732. https://doi.org/10.5194/bg-11-5707-2014

11. Capet, A., Stanev, E.V., Beckers, J.-M., Murray, J.W. and Grégoire, M., 2016. Decline of the Black Sea Oxygen Inventory. *Biogeosciences*, 13(4), pp. 1287-1297. https://doi.org/10.5194/bg-13-1287-2016

12. Ginzburg, A.I., Kostianoy, A.G., Nezlin, N.P., Soloviev, D.M. and Stanichny, S.V., 2002. Anticyclonic Eddies in the Northwestern Black Sea. *Journal of Marine Systems*, 32(1–3), pp. 91-106. https://doi.org/10.1016/S0924-7963(02)00035-0

13. Oguz, T., Deshpande, A.G. and Malanotte-Rizzoli, P., 2002. The Role of Mesoscale Processes Controlling Biological Variability in the Black Sea Coastal Waters: Inferences from SeaWIFS-Derived Surface Chlorophyll Field. *Continental Shelf Research*, 22(10), pp. 1477-1492. https://doi.org/10.1016/S0278-4343(02)00018-3

14. Kubryakov, A.A., Stanichny, S.V. and Zatsepin, A.G., 2018. Interannual Variability of Danube Waters Propagation in Summer Period of 1992–2015 and Its Influence on the Black Sea Ecosystem. *Journal of Marine Systems*, 179, pp. 10-30. https://doi.org/10.1016/j.jmarsys.2017.11.001

15. Belyaev, V.I. and Sovga, E.E., 1992. Mathematical Model for the Ecosystem of the Black Sea Hydrogen Sulphide Zone. *Soviet Journal of Physical Oceanography*, 3(6), pp. 455-470. https://doi.org/10.1007/BF02197560

16. Lyubartseva, S.P. and Lyubartsev, V.G., 1998. *Modeling of the Black Sea Anoxic Zone Processes*. NATO Science Series, 47(2), pp. 385-396.

17. Shushkina, E.A., Vinogradov, M.E., Lebedeva, L.P., Oguz, T., Nezlin, N.P., Dyakonov, V.Yu. and Anokhina, L.L., 1998. Studies of Structural Parameters of Planktonic Communities of the Open Part of the Black Sea Relevant to Ecosystem Modeling. In: L. I. Ivanov and T. Oguz, eds., 1998. *Ecosystem Modeling as a Management Tool for the Black Sea*. NATO Science Series 2 Environmental Security, vol. 47. Netherlands: Kluwer Academic Publishers. Vol. 1, pp. 311-326.

18. Lebedeva, L.P. and Shushkina, E.A., 1994. The Model Investigation of the Black Sea Plankton Community Changes Caused by Mnemiopsis. *Okeanologiya*, 34(1), pp. 79-87.

19. Oguz, T., Murray, J.W. and Callahan, A.E., 2001. Modeling Redox Cycling across the Suboxic–Anoxic Interface Zone in the Black Sea. *Deep Sea Research Part I: Oceanographic Research Papers*, 48(3), pp. 761-787. https://doi.org/10.1016/S0967-0637(00)00054-6

20. Oguz, T., Ducklow, H., Malanotte-Rizzoli, P., Tugrul, S., Nezlin, N.P. and Unluata, U., 1996. Simulation of Annual Plankton Productivity Cycle in the Black Sea by a One-Dimensional Physical-Biological Model. *Journal of Geophysical Research: Oceans*, 101(C7), pp. 16585-16599. https://doi.org/10.1029/96JC00831

21. Oguz, T., Ducklow, H.W. and Malanotte-Rizzoli, P., 2000. Modeling Distinct Vertical Biogeochemical Structure of the Black Sea: Dynamical Coupling of the Oxic, Suboxic, and Anoxic Layers. *Global Biogeochemical Cycles*, 14(4), pp. 1331-1352. https://doi.org/10.1029/1999GB001253

22. Staneva, J., Stanev, E. and Oguz, T., 1998. On the Sensitivity of the Planktonic Cycle to Physical Forcing. Model Study on the Time Variability of the Black Sea Ecological System. In: L. I. Ivanov and T. Oguz, eds., 1998. *Ecosystem Modeling as a Management Tool for the Black Sea*. NATO Science Partnership Subseries 2, vol. 47. Netherlands: Kluwer Academic Publishing. Vol. 2, pp. 301–322.

23. Grégoire, M. and Lacroix, G., 2003. Exchange Processes and Nitrogen Cycling on the Shelf and Continental Slope of the Black Sea Basin. *Global Biogeochemical Cycles*, 17(2), 1073. https://doi.org/10.1029/2002GB001882

24. Grégoire, M. and Friedrich, J., 2004. Nitrogen Budget of the Northwestern Black Sea Shelf Inferred from Modeling Studies and in Situ Benthic Measurements. *Marine Ecology Progress Series*, 270, pp.15-39. https://doi.org/10.3354/meps270015

25. Kubryakova, E.A., Kubryakov, A.A. and Stanichny, S.V., 2018. Impact of Winter Cooling on Water Vertical Entrainment and Intensity of Phytoplankton Bloom in the Black Sea. *Physical Oceanography*, 25(3), pp. 191-206. https://doi.org/10.22449/1573-160X-2018-3-191-206

26. Oguz, T. and Merico, A., 2006. Factors Controlling the Summer Emiliania Huxleyi Bloom in the Black Sea: A Modeling Study. *Journal of Marine Systems*, 59(3–4), pp. 173-188. https://doi.org/10.1016/j.jmarsys.2005.08.002

27. Dorofeev, V.L., Korotaev, G.K. and Sukhikh, L.I., 2012. Modeling of the Black Sea Ecosystem Evolution during Three Decades (1971–2001). *Morskoy Gidrofizicheskiy Zhurnal*, (3), pp. 61-74 (in Russian).

28. Grégoire, M. and Soetaert, K., 2010. Carbon, Nitrogen, Oxygen and Sulfide Budgets in the Black Sea: A Biogeochemical Model of the Whole Water Column Coupling the Oxic and Anoxic Parts. *Ecological Modelling*, 221(19), pp. 2287-2301. https://doi.org/10.1016/j.ecolmodel.2010.06.007

29. Mikaelyan, A.S., Malej, A., Shiganova, T.A., Turk, V., Sivkovitch, A.E., Musaeva, E.I., Kogovšek, T. and Lukasheva, T.A., 2014. Populations of the Red Tide Forming Dinoflagellate Noctiluca Scintillans (Macartney): A Comparison between the Black Sea and the Northern Adriatic Sea. *Harmful Algae*, 33, pp. 29-40. https://doi.org/10.1016/j.hal.2014.01.004

30. Konovalov, S.K. and Murray, J.W., 2001. Variations in the Chemistry of the Black Sea on a Time Scale of Decades (1960–1995). *Journal of Marine Systems*, 31(1–3), pp. 217-243. https://doi.org/10.1016/S0924-7963(01)00054-9

31. Yakushev, E.V., Lukashev, Yu.F., Chasovnikov, V.K. and Chzhu, V.P., 2002. Modern Notion of Redox Zone Vertical Hydrochemical Structure in the Black Sea. In: Zatsepin, A.G. and Flint, M.V., eds., 2002. *Multidisciplinary Investigations of the Northeast Part of the Black Sea*. Moscow: Nauka, pp. 119-133 (in Russian).

32. Konovalov, S.K., Murray, J.W., Luther, G.W. and Tebo, B.M., 2006. Processes Controlling the Redox Budget for the Oxic/Anoxic Water Column of the Black Sea. *Deep Sea Research Part II: Topical Studies in Oceanography*, 53(17–19), pp. 1817-1841. https://doi.org/10.1016/j.dsr2.2006.03.013

33. Kubryakova, E.A. and Korotaev, G.K., 2016. Influence of Vertical Motions on Maintaining the Nitrate Balance in the Black Sea Based on Numerical Simulation. *Oceanology*, 56(1), pp. 25-35. https://doi.org/10.1134/S0001437016010082

34. Di Biagio, V., Cossarini, G., Salon, S., Lazzari, P., Querin, S., Sannino, G. and Solidoro, C., 2019. Temporal Scales of Variability in the Mediterranean Sea Ecosystem: Insight from a Coupled Model. *Journal of Marine Systems*, 197, 103176. https://doi.org/10.1016/j.jmarsys.2019.05.002

35. Edman, M.K. and Anderson, L.G., 2014. Effect on pCO2 by Phytoplankton Uptake of Dissolved Organic Nutrients in the Central and Northern Baltic Sea, a Model Study. *Journal of Marine Systems*, 139, pp. 166-182. https://doi.org/10.1016/j.jmarsys.2014.06.004

36. Chernov, I., Lazzari, P., Tolstikov, A., Kravchishina, M. and Iakovlev, N., 2018. Hydrodynamical and Biogeochemical Spatiotemporal Variability in the White Sea: A Modeling Study. *Journal of Marine Systems*, 187, pp. 23-35. https://doi.org/10.1016/j.jmarsys.2018.06.006

37. Chernov, I. and Tolstikov, A., 2020. The White Sea: Available Data and Numerical Models. *Geosciences*, 10(11), 463. https://doi.org/10.3390/geosciences10110463

38. Mizyuk, A.I. and Korotaev, G.K., 2020. Black Sea Intrapycnocline Lenses According to the Results of a Numerical Simulation of Basin Circulation. *Izvestiya, Atmospheric and Oceanic Physics*, 56(1), pp. 92-100. https://doi.org/10.1134/S0001433820010107

39. Kubryakov, A.A., Mizyuk, A.I. and Stanichny, S.V., 2024. Stationarity and Separation of the Sevastopol Eddies in the Black Sea: The Role of Eddy-Topographic Interaction and Submesoscale Dynamics. *Journal of Marine Systems*, 241, 103911. https://doi.org/10.1016/j.jmarsys.2023.103911

40. Mizyuk, A.I., Korotaev, G.K., Grigoriev, A.V., Puzina, O.S. and Lishaev, P.N., 2019. Long-Term Variability of Thermohaline Characteristics of the Azov Sea Based on the Numerical Eddy-Resolving Model. *Physical Oceanography*, 26(5), pp. 438-450. https://doi.org/10.22449/1573-160X-2019-5-438-450

41. Kubryakov, A.A., Mizyuk, A.I., Puzina, O.S. and Senderov, M.V., 2018. Three-Dimensional Identification of the Black Sea Mesoscale Eddies According to NEMO Numerical Model Calculations. *Physical Oceanography*, (1), pp. 18-26. https://doi.org/10.22449/1573-160X-2018-1-18-26

42. Hersbach, H., Bell, B., Berrisford, P., Hirahara, S., Horányi, A., Muñoz-Sabater, J., Nicolas, J., Peubey, C., Radu, R. [et al.], 2020. The ERA5 Global Reanalysis. *Quarterly Journal of the Royal Meteorological Society*, 146(730), pp. 1999-2049. https://doi.org/10.1002/qj.3803

43. Vichi, M., Pinardi, N. and Masina, S., 2007. A Generalized Model of Pelagic Biogeochemistry for the Global Ocean Ecosystem. Part I: Theory. *Journal of Marine Systems*, 64(1–4), pp. 89-109. https://doi.org/10.1016/j.jmarsys.2006.03.006

44. Man'kovsky, V.I. and Solov'ev, M.V., 2003. Optical Characteristics of the Black Sea Water in 1922–1985 (Climatic Maps). *Ecological Safety of Coastal and Shelf Zones of Sea*, 8, pp. 23-47 (in Russian).

45. Jassby, A.D. and Platt, T., 1976. Mathematical Formulation of the Relationship between Photosynthesis and Light for Phytoplankton. *Limnology and Oceanography*, 21(4), pp. 540-547. https://doi.org/10.4319/lo.1976.21.4.0540

46. Soetaert, K., Middelburg, J.J., Herman, P.M.J. and Buis, K., 2000. On the Coupling of Benthic and Pelagic Biogeochemical Models. *Earth-Science Reviews*, 51(1–4), pp. 173-201. https://doi.org/10.1016/S0012-8252(00)00004-0

47. Miladinova, S., Stips, A., Macias Moy, D. and Garcia-Gorriz, E., 2020. Seasonal and Inter-Annual Variability of the Phytoplankton Dynamics in the Black Sea Inner Basin. *Oceans*, 1(4), pp. 251-273. https://doi.org/10.3390/oceans1040018

48. Kawamiya, M., Kishi, M.J. and Suginohara, N., 2000. An Ecosystem Model for the North Pacific Embedded in a General Circulation Model: Part I: Model Description and Characteristics of Spatial Distributions of Biological Variables. *Journal of Marine Systems*, 25(2), pp. 129-157. https://doi.org/10.1016/S0924-7963(00)00012-9

49. Leonard, C.L., McClain, C.R., Murtugudde, R., Hofmann, E.E. and Harding, L.W., 1999. An Iron-Based Ecosystem Model of the Central Equatorial Pacific. *Journal of Geophysical Research: Oceans*, 104(C1), pp. 1325-1341. https://doi.org/10.1029/1998JC900049

50. Finenko, Z.Z., Churilova, T.Y., Sosik, H.M. and Basturk, O., 2002. Variability of Photosynthetic Parameters of the Surface Phytoplankton in the Black Sea. *Oceanology*, 42(1), pp. 53-67.

51. Christian, J.R., Verschell, M.A., Murtugudde, R., Busalacchi, A.J. and McClain, C.R., 2001. Biogeochemical Modelling of the Tropical Pacific Ocean. I: Seasonal and Interannual Variability. *Deep Sea Research Part II: Topical Studies in Oceanography*, 49(1–3), pp. 509-543. https://doi.org/10.1016/S0967-0645(01)00110-2

52. Baretta-Bekker, J.G., Baretta, J.W. and Rasmussen, E.K., 1995. The Microbial Food Web in the European Regional Seas Ecosystem Model. *Netherlands Journal of Sea Research*, 33(3–4), pp. 363-379. https://doi.org/10.1016/0077-7579(95)90053-5

53. Broekhuizen, N., Heath, M.R., Hay, S.J. and Gurney, W.S.C., 1995. Modelling the Dynamics of the North Sea's Mesozooplankton. *Netherlands Journal of Sea Research*, 33(3–4), pp. 381-406. https://doi.org/10.1016/0077-7579(95)90054-3

54. Stel'makh, L.V., Babich, I.I., Tugrul, S., Moncheva, S. and Stefanova, K., 2009. Phytoplankton Growth Rate and Zooplankton Grazing in the Western Part of the Black Sea in the Autumn Period. *Oceanology*, 49(1), pp. 83-92. https://doi.org/10.1134/S000143700901010X

55. Stelmakh, L. and Georgieva, E., 2014. Microzooplankton: The Trophic Role and Involvement in the Phytoplankton Loss and Bloom-Formation in the Black Sea. *Turkish Journal of Fisheries and Aquatic Sciences*, 14, pp. 955-964. http://dx.doi.org/10.4194/1303-2712-v14_4_15

56. Stelmakh, L.V., 2013. Microzooplankton Grazing Impact on Phytoplankton Blooms in the Coastal Seawater of the Southern Crimea (Black Sea). *International Journal of Marine Science*, 3(15), pp. 121-127. https://doi.org/10.5376/ijms.2013.03.0015

57. Vichi, M., Oddo, P., Zavatarelli, M., Coluccelli, A., Coppini, G., Celio, M., Fonda Umani, S. and Pinardi, N., 2003. Calibration and Validation of a One-Dimensional Complex Marine Biogeochemical Flux Model in Different Areas of the Northern Adriatic Shelf. *Annales Geophysicae*, 21(1), pp. 413-436. https://doi.org/10.5194/angeo-21-413-2003

58. Vichi, M., Ruardij, P. and Baretta, J.W., 2004. Link or Sink: A Modelling Interpretation of the Open Baltic Biogeochemistry. *Biogeosciences*, 1, pp. 79-100. https://doi.org/10.5194/bgd-1-219-2004

59. Tyrrell, T. and Merico, A., 2004. Emiliania Huxleyi: Bloom Observations and the Conditions That Induce Them. In: H. R. Thierstein, and J. R. Young, eds., 2004. *Coccolithophores*. Berlin, Heidelberg: Springer, pp. 75-97. https://doi.org/10.1007/978-3-662-06278-4_4

60. Benner, I. and Passow, U., 2010. Utilization of Organic Nutrients by Coccolithophores. *Marine Ecology Progress Series*, 404, pp. 21-29. https://doi.org/10.3354/meps08474

61. Godrijan, J., Drapeau, D. and Balch, W.M., 2020. Mixotrophic Uptake of Organic Compounds by Coccolithophores. *Limnology and Oceanography*, 65(6), pp. 1410-1421. https://doi.org/10.1002/lno.11396

62. De Lange, H.J., Morris, D.P. and Williamson, C.E., 2003. Solar Ultraviolet Photodegradation of DOC May Stimulate Freshwater Food Webs. *Journal of Plankton Research*, 25(1), pp. 111-117. https://doi.org/10.1093/plankt/25.1.111

63. Weiss, R.F., 1970. The Solubility of Nitrogen, Oxygen and Argon in Water and Seawater. *Deep Sea Research and Oceanographic Abstracts*, 17(4), pp. 721-735. https://doi.org/10.1016/0011-7471(70)90037-9

64. Yakushev, E.V., Pollehne, F., Jost, G., Kuznetsov, I., Schneider, B. and Umlauf, L., 2007. Analysis of the Water Column Oxic/Anoxic Interface in the Black and Baltic Seas with

a Numerical Model. *Marine Chemistry*, 107(3), pp. 388-410. https://doi.org/10.1016/j.marchem.2007.06.003

65. Dorofeev, V.L. and Sukhikh, L.I., 2019. [Assessment of the Influence of the Black Sea Circulation on Nutrient Fluxes from the Shelf to the Central Part Based on Reanalysis Results]. In: MHI RAS, 2019. *Seas of Russia: Fundamental and Applied Research: Abstracts of the All-Russian Scientific Conference*. Sevastopol, p. 70 (in Russian).
66. Khaliulin, A.Kh., Godin, E.A., Ingerov, A.V., Zhuk, E.V., Galkovskaya, L.K. and Isaeva, E.A., 2016. Ocean Data Bank of the Marine Hydrophysical Institute: Information Resources to Support Research in the Black Sea Coastal Zone. *Ecological Safety of Coastal and Shelf Zones of Sea*, (1), pp. 82-89 (in Russian).
67. Zatsepin, A.G., Ginzburg, A.I., Kostianoy, A.G., Kremenetskiy, V.V., Krivosheya, V.G., Stanichny, S.V. and Poulain, P.-M., 2003. Observations of Black Sea Mesoscale Eddies and Associated Horizontal Mixing. *Journal of Geophysical Research: Oceans*, 108(C8), 3246. https://doi.org/10.1029/2002JC001390
68. Kubryakov, A.A., Stanichny, S.V., Zatsepin, A.G. and Kremenetsky, V.V., 2016. Long-Term Variations of the Black Sea Dynamics and Their Impact on the Marine Ecosystem. *Journal of Marine Systems*, 163, pp. 80-94. https://doi.org/10.1016/j.jmarsys.2016.06.006
69. Svishchev, S.V. and Kubryakov, A.A., 2022. Impact of Winter Cooling on the Interannual Variability in the Vertical Oxygen Distribution in the Black Sea: Evidence from Bio-Argo Floats. *Oceanology*, 62(2), pp. 143-154. https://doi.org/10.1134/S0001437022020163
70. Kubryakova, E.A., Kubryakov, A.A. and Mikaelyan, A.S., 2021. Winter Coccolithophore Blooms in the Black Sea: Interannual Variability and Driving Factors. *Journal of Marine Systems*, 213, 103461. https://doi.org/10.1016/j.jmarsys.2020.103461
71. Kubryakov, A.A., Belokopytov, V.N., Zatsepin, A.G., Stanichny, S.V. and Piotukh, V.B., 2019. The Black Sea Mixed Layer Depth Variability and Its Relation to the Basin Dynamics and Atmospheric Forcing. *Physical Oceanography*, 26(5), pp. 397-413. https://doi.org/10.22449/1573-160X-2019-5-397-413
72. Stelmakh, L.V., 2018. Environmental and Physiological Bases of Coccolithophorid Emiliania Huxleyi Spring Bloom Development in the Black Sea. *Monitoring Systems of Environment,* 13, pp. 85-92. https://doi.org/10.33075/2220-5861-2018-3-85-92 (in Russian).
73. Vedernikov, V.I. and Demidov, A.B., 1993. Primary Production and Chlorophyll in the Deep-Sea Regions of the Black Sea. *Oceanology*, 33(2), pp. 229-235 (in Russian).
74. Ricour, F., Capet, A., D'Ortenzio, F., Delille, B. and Grégoire, M., 2021. Dynamics of the Deep Chlorophyll Maximum in the Black Sea as Depicted by BGC-Argo Floats. *Biogeosciences*, 18(2), pp. 755-774. https://doi.org/10.5194/bg-18-755-2021

Submitted 28.09.2023; approved after review 06.06.2025;
accepted for publication 10.11.2025.

About the authors:

Pavel N. Lishaev, Researcher, Marine Hydrophysical Institute of RAS (2 Kapitanskaya Str., Sevastopol, 299011, Russian Federation), CSc. (Phys.-Math.), **SPIN-code: 2241-1505**, **Scopus Author ID: 57193071072**, **WoS ResearcherID: A-7770-2019**, **ORCID ID: 0000-0002-5259-3309**, pavellish@mail.ru

Elena A. Kubryakova, Senior Researcher, Marine Hydrophysical Institute of RAS (2 Kapitanskaya Str., Sevastopol, 299011, Russian Federation), CSc. (Phys.-Math.), **SPIN-code: 7946-8985**, **Scopus Author ID: 57188747330**, **WoS ResearcherID: G-1433-2014**, **ORCID ID: 0000-0001-6071-1881**, elena_kubryakova@mail.ru

Arseny A. Kubryakov, Deputy Director for Scientific Affairs, Marine Hydrophysical Institute of RAS (2 Kapitanskaya Str., Sevastopol, 299011, Russian Federation), DSc. (Phys.-Math.), **SPIN-code: 4371-8879**, **Scopus Author ID: 37072750100**, **WoS ResearcherID: F-8921-2014**, **ORCID ID: 0000-0003-3561-5913**, arskubr@yandex.ru

Contribution of the co-authors:

Pavel N. Lishaev – formulation of goals and objectives of the study, mathematical model refinement, conducting numerical experiments, processing and description of the research results, text preparation, editing and revision of the article

Elena A. Kubryakova – formulation of goals and objectives of the study, mathematical model refinement, processing and description of the research results, text preparation

Arseny A. Kubryakov – formulation of goals and objectives of the study, qualitative analysis of the results and their interpretation, processing and description of the research results, text preparation

The authors have read and approved the final manuscript.
The authors declare that they have no conflict of interest.